

Long-term magnetic activity of a sample of M-dwarf stars from the HARPS program[★]

II. Activity and radial velocity

J. Gomes da Silva^{1,2}, N.C. Santos^{1,2}, X. Bonfils³, X. Delfosse³, T. Forveille³, S. Udry⁴, X. Dumusque^{1,4}, and C. Lovis⁴

¹ Centro de Astrofísica, Universidade do Porto, Rua das Estrelas, 4150-762 Porto, Portugal
e-mail: Joao.Silva@astro.up.pt

² Departamento de Física e Astronomia, Faculdade de Ciências, Universidade do Porto, Portugal

³ UJF-Grenoble 1 / CNRS-INSU, Institut de Planétologie et d'Astrophysique de Grenoble (IPAG) UMR 5274, Grenoble, F-38041, France

⁴ Observatoire de Genève, Université de Genève, 51 ch. des Maillettes, CH-1290 Versoix, Switzerland

Preprint online version: July 30, 2018

ABSTRACT

Due to their low mass and luminosity, M dwarfs are ideal targets if one hopes to find low-mass planets similar to Earth by using the radial velocity (RV) method. However, stellar magnetic cycles could add noise or even mimic the RV signal of a long-period companion. Following our previous work that studied the correlation between activity cycles and long-term RV variations for K dwarfs we now expand that research to the lower-end of the main sequence. Our objective is to detect any correlations between long-term activity variations and the observed RV of a sample of M dwarfs. We used a sample of 27 M-dwarfs with a median observational timespan of 5.9 years. The cross-correlation function (CCF) with its parameters RV, bisector inverse slope (BIS), full-width-at-half-maximum (FWHM) and contrast have been computed from the HARPS spectrum. The activity index have been derived using the Na I D doublet. These parameters were compared with the activity level of the stars to search for correlations. We detected RV variations up to $\sim 5 \text{ m s}^{-1}$ that we can attribute to activity cycle effects. However, only 36% of the stars with long-term activity variability appear to have their RV affected by magnetic cycles, on the typical timescale of ~ 6 years. Therefore, we suggest a careful analysis of activity data when searching for extrasolar planets using long-timespan RV data.

Key words. Planetary systems - Techniques: spectroscopic - Techniques: radial velocities - Stars: activity - Stars: late-type

1. Introduction

The majority of extrasolar planets discovered so far were either detected or confirmed via the radial velocity method¹. This technique measures the Doppler effect due to the wobble of the star around the centre of mass of the star-planet system. As an indirect method, it is sensitive to stellar sources of noise like oscillations, granulation, rotating active regions, and magnetic cycles.

Stellar oscillations and granulation induce radial velocity variations on timescales up to some hours and can easily be suppressed if a optimized observational strategy is used (Dumusque et al. 2011b). However, this is not true for the case of rotationally modulated active regions which have longer timescales. The effect of rotating active regions on line profiles, and hence RV measurements, can easily hide or mimic the signal of orbiting companions (e.g. Saar & Donahue 1997; Santos et al. 2000; Queloz et al. 2001). In some cases, these effects can be diagnosed e.g. by the anti-correlation between instantaneous measurements of RV and the bisector inverse slope (Queloz et al. 2001; Boisse et al. 2011) and corrected by subtracting the anti-correlation slope to the RV measurements (e.g. Melo et al. 2007; Boisse et al. 2009) or by fitting an extra Keplerian orbit to the

RV data with the period detected in the activity time-series (e.g. Bonfils et al. 2007; Forveille et al. 2009). Queloz et al. (2009) and Boisse et al. (2011) proposed to fit the activity signal with sinusoids of different periods: the rotation one and its harmonics. Saar & Fischer (2000) used a different technique to correct for long-term activity induced RV. These authors used the slope of the S_{IR} -RV correlation to remove the activity influence from the radial velocity signal.

Long-term stellar magnetic cycles can also be a source of noise for precise RV measurements. Kürster et al. (2003) studied the correlation between radial velocity and the H α index for the nearby Barnard's star (Gl 699). They found an anti-correlation between velocity and the activity index with a correlation coefficient of $\rho = -0.50$. The authors concluded that activity as measured by the hydrogen line was producing a blueshift of the photospheric absorption lines.

By using simulations, Meunier et al. (2010) showed that magnetic activity cycles can induce radial-velocity variations for the case of the Sun as seen edge-on with amplitudes that can reach the $\sim 10 \text{ m s}^{-1}$ level. These kind of variations in a star with a periodic activity cycle could be able to mimic the signal of a long-period extra-solar planet.

In this context, Santos et al. (2010) used a sample of 8 solar-type stars with the aim of studying if a correlation between long term activity and RV variations exists. The long-term variations were detected on the S_{MW} , H α , and He I indices and the BIS,

[★] Based on observations made with the HARPS instrument on the ESO 3.6-m telescope at La Silla Observatory under programme ID 072.C-0488(E)

¹ cf. <http://exoplanet.eu/>

FWHM and contrast CCF parameters but only two stars showed correlations with RV stronger than $\rho > |0.75|$: one positive correlation and one anti-correlation. The authors concluded then that the possible amplitudes of induced RV variations for the early-K dwarfs was low, at the $\sim 1 \text{ m s}^{-1}$ level similar to the HARPS precision.

Using a larger sample of around 300 stars from the HARPS FGK high precision program, Lovis et al. (2011) studied the correlation between long-term activity variations with radial-velocity in a similar fashion as Santos et al. (2010) did. They found a correlation between the slope of the RV–activity index (R'_{HK}) correlation, effective temperature (T_{eff}), and metallicity ($[\text{Fe}/\text{H}]$). The slope is weaker for late-type dwarfs than for early ones and therefore, it seems that the RVs of later-K dwarfs are less affected by magnetic cycles than the RVs of early-G dwarfs. Therefore, the influence of long-term activity could be corrected if the activity level, effective temperature and metallicity of the star are known by using the slope of the RV– $\log(R'_{HK})$ relation.

Hints of long term RV variations produced by activity cycles were found by Moutou et al. (2011) in the stars BD-114672 and HIP21934, with periods of 1692 and 1100 days respectively. Ségransan et al. (2011) also found a long term period of ~ 500 days on the radial velocity of HD104067 (K2V). The activity index of this star, hosting a 55-day period Neptune-like planet, was found to have a correlation with the RV residuals (with $\sigma_{RV} = 4.6 \text{ m s}^{-1}$) after the planetary signal was removed.

More recently, three exoplanets were discovered in three early-K stars with magnetic cycles by correcting the activity signals in the radial velocity data (Dumusque et al. 2011a). The planets were found by fitting simultaneously two keplerians: one for the planet and one for the magnetic cycle. All the parameters of the keplerian fitting the cycle, except the amplitude, were fixed to the ones obtained when fitting the activity index only. This proves that (i) magnetic activity cycles of stars can influence radial velocity *and* hide the signal of long-period planets, and (ii) a correction of the long-term activity-induced RV is possible and can be used to recover the embedded signal of a planet.

In Gomes da Silva et al. (2011, hereafter Paper I) we compared the long-term activity variations using four activity indices for a sample of M-dwarf stars from the HARPS program. We arrived to the conclusion that the Na I index was the most appropriate of the four to study the activity of these type of stars. We will now use in this paper the Na I index as the proxy of activity with the aim of comparing long-term activity to RV and some other relevant CCF parameters using the same sample of stars. This paper will therefore extend the first study in Santos et al. (2010) to the case of early-M dwarfs.

This paper is organised as follows: in Sect. 2 we present our sample and observation log and explain our data analysis, in Sect 3 a selection of a subsample of stars with long-term activity variability is done, in Sect. 4 we determine which stars have hints of periodic magnetic cycles, in Sect. 5 we compare long-term activity with radial velocity and the CCF parameters, in Sect. 6 we examine individual stars with strong activity-RV correlation and other interesting cases, and finally in Sect. 7 we draw our conclusions from the present work.

2. Sample and observations

The sample we are using comes from the HARPS M-dwarf planet search program that started in 2003 and ended in 2009 (see Bonfils et al. 2011). We used this sample in Paper I to study four known chromospheric activity indices and to select stars with long-term activity variability. However, we now use more

data that were taken in 2010 as part of the Bonfils et al. (2011) program extension. Therefore, We decided to redo the same analysis as in Paper I using the new data to detect any new cases of activity variability that could arise from more data points.

We obtained simultaneous radial-velocity, BIS, FWHM, contrast, and the Na I activity indicator. The median radial-velocity error of the nightly averaged data was 1.2 m s^{-1} . HARPS is capable of more precise measurements (e.g. Mayor et al. 2011) but our sample includes dim stars which make it more difficult to get high signal-to-noise ratios (SNR) and therefore higher-precision RVs. To measure activity² we used the index based on the Na I D1 and D2 lines in a same way as in Paper I (see also Díaz et al. 2007a). The CCF parameters were used because of their potential as complementary long-term activity proxies (e.g. Santos et al. 2010).

Because of an instrumental drift detected on HARPS that affected the FWHM and contrast of the CCF, these parameters were corrected using the following expressions:

$$FWHM_{\text{corr}} = FWHM + 5.66 \cdot 10^{-6}D - 1.77 \cdot 10^{-9}D^2 \quad (1)$$

$$\text{contrast}_{\text{corr}} = \text{contrast} + 4.59 \cdot 10^{-5}D - 2.75 \cdot 10^{-8}D^2 \quad (2)$$

where D is $(BJD - 2454500)$ days. However, this correction is very small and is a long-term drift. For example the FWHM drift is only 0.1% in five years.

Since this sample includes some stars very close to the Sun, these stars may have significant secular acceleration that could produce a trend on the observed radial-velocity. We corrected all stars for this effect using the proper motions and parallaxes that were retrieved from the Hipparcos catalog (ESA 1997). The secular accelerations were calculated following the description in Zechmeister et al. (2009) and the radial-velocities subsequently corrected (see also Bonfils et al. 2011).

Some of the stars in this sample are planet hosts, namely G1 176, G1 433, G1 436, G1 581, G1 667 C, G1 674, G1 832, G1 849, G1 876, HIP12961, and HIP85647 (Bonfils et al. 2011). Because we are only interested in variations due to activity, these planetary signals were subtracted from the observed radial-velocities by fitting keplerian functions based on the published orbital parameters.

The selection criteria was the same as in our previous paper. We nightly averaged and binned the data into 150-day bins to average out short time-scale variability, since we are only concerned with long-term variations. Only bins with more than three nights and stars with at least four bins were selected. The errors used for each bin are the statistical errors on the average, $\sigma_i = \sigma / \sqrt{N}$, where σ is the root-mean-square (rms) of the nightly averaged data in each bin, and N is the number of nights included in the bin.

We also decided to select only stars with at least three years of observations, which resulted in GJ 361, GJ 2049, and GJ 3218 being discarded from the sample. This resulted in a sample of 27 stars which passed the selection criteria, whose basic parameters are presented in Table 1. These stars have spectral types in the range M0–M5.5 V and have V magnitudes between 7.34 and 11.81. In the same table we also present the observation log, with information about the number of nights of observation, the timespan in days and years, the average signal-to-noise ratio at spectral order 56 (the order of the Na I doublet, $\sim 5893\text{\AA}$) and the average radial-velocity error. The timespan of the observations range from 3.3 to 7.2 years (with a median value of 5.9 years).

² From now on we will use the terms activity, Na I, and sodium lines interchangeably.

Table 1: Basic parameters and observation log of the sample.

Star	Other names	Sp. Type ^a	V^d [mag]	$V - I^e$ [mag]	$BJD_{start} - 2400000$ [days]	# nights	T_{span} [days]	$\langle S/N \rangle$ (order 56)	$\langle \sigma_i(V_r) \rangle$ [m s ⁻¹]
Gl 1		M3V	8.57	2.13	52985.60	45	2063	95.6	0.7
Gl 176 [†]		M2.5V	9.97	2.25	52986.71	71	2146	47.6	1.2
Gl 205		M1.5V	7.92	2.08	52986.73	75	1400	108.5	0.8
Gl 273		M3.5V	9.89	2.71	52986.77	62	2140	57.3	0.8
Gl 382		M2V	9.26	2.18	52986.84	30	1188	66.7	1.1
Gl 393		M2V	9.76	2.26	52986.86	29	1897	67.0	1.0
Gl 433 [†]		M2V	9.79	2.15	52989.84	61	2245	56.6	1.2
Gl 436 [†]		M2.5V ^b	10.68	2.02	53760.83	115	1532	32.9	1.4
Gl 479		M3V	10.64	1.90	53158.55	58	1413	43.3	1.2
Gl 526		M1.5V	8.46	2.07	53158.60	34	1843	101.6	0.8
Gl 551	Prox Cent	M5.5V	11.05	3.62	53152.60	42	2140	21.1	1.3
Gl 581 [†]		M2.5V	10.57	2.53	53152.71	194	2306	36.4	1.2
Gl 588		M2.5V	9.31	2.40	53152.75	32	2200	75.4	0.8
Gl 667 C [†]		M2V	10.22	2.08	53158.76	173	2201	42.9	1.3
Gl 674 [†]		M3V	9.36	2.40	53158.75	44	1574	70.6	0.8
Gl 680		M1.5V	10.14	2.27	53159.71	35	2269	41.2	1.4
Gl 699	Barnard's star	M4V	9.54	2.52	54194.89	32	1291	34.3	0.8
Gl 832 [†]		M1V	8.67	2.18	52985.52	59	2424	88.9	0.8
Gl 849 [†]		M3V	10.42	2.50	52990.54	49	2423	41.9	1.3
Gl 876 [†]		M3.5V	10.17	2.77	52987.58	67	2508	42.6	1.1
Gl 877		M2.5V	10.55	2.43	52857.83	40	2636	36.5	1.2
Gl 887		M2V	7.34	2.02	52985.57	63	1407	131.3	0.8
Gl 908		M1V	8.98	2.04	52986.58	66	2511	76.0	0.9
HIP12961 [†]		M0V ^c	9.7	1.64	52991.63	46	2226	46.5	3.0
HIP19394		M3.5V ^d	11.81	2.5	52942.80	35	2495	23.3	2.0
HIP38594		M ^d	9.96	1.64	52989.79	17	2229	41.1	2.0
HIP85647 [†]	GJ 676 A	M0V ^b	9.59	1.85	53917.75	38	1520	36.6	2.4

Notes. The average radial-velocity errors, $\langle \sigma_i(V_r) \rangle$, are taken after removal of the planetary companion's signals. (†) Stars with published planetary companions.

References. (a) Bonfils et al. (2011) unless individually specified; (b) Hawley et al. (1996); (c) Koen et al. (2010); (d) Simbad (<http://simbad.u-strasbg.fr/simbad/>); (e) ESA (1997)

The average errors on radial velocity per star for the nightly averaged data vary between 0.8 and 3.0 m s⁻¹.

3. Na I index variability

In Paper I we compared four activity indices, namely S_{CaII} , $H\alpha$, Na I, and He I, and arrived to the conclusion that the Na I index is the best to follow the long-term activity of M-dwarf stars. We also tested our sample for variability and found that Gl 1, Gl 273, Gl 433, Gl 436, Gl 581, Gl 588, Gl 667 C, Gl 832, Gl 849, Gl 877, Gl 908, and HIP85647 showed significant ($P(F) \leq 0.05$) long-term activity variability on at least two indices. However, we are now using the latest data with new measurements from 2010 (previously we used data covering the years 2003–2009) and consequently other stars might now show statistical variability on long time-scale activity that was not detected before. We therefore decided to repeat the variability F-tests, this time using only the Na I index.

The Na I activity proxy was determined as explained in Paper I, by measuring the flux in the centre of the sodium D1 and D2 lines in comparison to the flux on two reference bands. This index is not calibrated to the bolometric flux of the stars and therefore it will depend on the effective temperature of each star (see discussion on Sect. 6.6 of Paper I). As a consequence, this index cannot be used to compare the activity of stars with different effective temperatures. Nevertheless, it can be used to detect activity variability with time for a given star.

In a similar fashion to what was done in Paper I, we asked whether the long time-scale variations observed in our data were of statistical significance. As previously done in Paper I, we used the F-test with an F-value as $F = \sigma_e^2 / \langle \sigma_i \rangle^2$ where σ_e is the standard deviation and $\langle \sigma_i \rangle$ the average of the error on the mean of the binned parameter for each star (see Endl et al. 2002; Zechmeister et al. 2009; Bonfils et al. 2011). This F-test will give the probability that the observed standard deviation can be explained by the random scatter due to the internal errors. Therefore, a low value of $P(F)$ will discriminate the stars which have significant variability not justified by the internal errors. The results of these tests are shown in Table 2. Bold values indicate probabilities lower than 0.05 (95% significance level). The F-value used to calculate the probabilities was $F = \sigma_e(\text{Na I})^2 / \langle \sigma_i(\text{Na I}) \rangle^2$ where σ_e stands for the rms of the (binned) data and $\langle \sigma_i \rangle$ is the average of the error on the mean. Also shown is the number of bins N_{bins} , indication if the star passed the variability tests in Paper I, *See*, the radial-velocity's rms $\langle \sigma_e(V_r) \rangle$ and average error on the mean $\langle \sigma_i(V_r) \rangle$, and the average value of the Na I index, $\langle \text{Na I} \rangle$.

Fourteen out of the 27 stars show long-term activity variability with $P(F) \leq 0.05$, representing 52% of the sample. These stars are Gl 273, Gl 433, Gl 436, Gl 526, Gl 581, Gl 588, Gl 667 C, Gl 699, Gl 832, Gl 849, Gl 876, Gl 877, Gl 908, and HIP85647. These are the same stars that passed the tests in Paper I plus Gl 526, Gl 699, and Gl 876, and less Gl 1. Four more stars, Gl 680, Gl 887, HIP19394, and HIP38594, have $0.05 < P(F) \leq$

0.1, which if they are considered increases the percentage of stars with variability to 67%. In Paper I we found 17 stars out of 30 showing variability in the Na I index with $P(F) \leq 0.1$, representing 57 % of the sample. This represents an increase of variable stars by 10% from our previous work just by adding one more year of observations, and thus, more of these stars could show long-term variability if a longer time-span is considered. We should note that Gl 1 passed the variability test on Paper I but not here. This is because on Paper I this star passed the test due to its variability in the $S_{\text{Ca II}}$ and $H\alpha$ indices, while not showing significant variability in Na I. Since we used only this index now and Gl 1 have not had more data points in 2010, this star now failed to pass the F-test based just on Na I.

By using a sample of old FGK stars in the solar neighbourhood studied for up to 7 years, Lovis et al. (2011) found that 61% have a magnetic activity cycle. Although we cannot confirm the cyclic nature of our detected long-term activity variations, our results are compatible with those of Lovis et al. (2011).

From now on we will consider only these 14 stars for the rest of the study, unless specified.

4. Activity cycle fits

Some stars show clear long-term variation of their activity, well visible with a general trend (increase or decrease of activity during several observational seasons). These include stars that have not passed the variability F-tests of Sect. 3. There is evidence that the periodic activity cycles of M-dwarf stars can be well fitted by a sinusoidal function (see Cincunegui et al. 2007; Díaz et al. 2007b; Buccino et al. 2011). Given the usually reduced number of points in our study, fitting other functions (e.g. Keplerian) would not bring further constraints since it would increase the number of free fitting parameters close to the number of data points. We therefore tried to fit a sinusoidal signal to Na I data to obtain the periods of such cycles (minimum periods for the cases of data covering less than one period). The fitted sinusoidal signal was of the form

$$\text{Na I}_{\text{ine}} = A \sin\left(\frac{2\pi}{P_{\text{cycle}}}t + \phi\right) + \delta, \quad (3)$$

where A is the semi-amplitude in units of Na I, P_{cycle} the activity cycle period in days, t the observation epoch in days, ϕ the phase, and δ a constant offset. The quality of the fit was obtained by a p-value, which gives the probability that the data is better fit by a straight line than by a sinusoidal signal. This p-value was calculated via an F-value given by

$$F(\chi^2) = (N - 4) \frac{\chi_{\text{line}}^2 - \chi_{\text{sine}}^2}{\chi_{\text{sine}}^2}, \quad (4)$$

where *line* and *sine* identify if the model used was the linear fit or sinusoidal fit, respectively, and N is the number of data points. The chi-squared function used was

$$\chi^2 = \sum_{i=1}^N \left[\frac{\text{Na I}_n - \text{Na I}_{n,\text{sine}}}{\sigma_i(\text{Na I})_n} \right]^2, \quad \text{for } 1 \leq n \leq N, \quad (5)$$

where Na I_n are the observed values of the activity index, $\text{Na I}_{n,\text{sine}}$ are the activity values obtained from the fitted *sine* model, and $\sigma_i(\text{Na I})_n$ the internal errors of each individual Na I_n. Smaller p-values will indicate that the data was better fitted by a sinusoid. Note that these fits were carried out without taking in consideration whether the star passed the variability F-tests in

Sect. 3 or not. Also, it is only possible to calculate the probabilities for the stars which have five or more data points, otherwise $(N - 4) \leq 0$. Eight stars had their long-term activity successfully fitted by a sinusoidal signal, with $P(\chi^2) \leq 0.1$. These stars are Gl 1, Gl 382, Gl 433, Gl 581, Gl 667 C, Gl 680, Gl 832, and HIP85647. However, Gl 1, Gl 382, and Gl 680 have not passed the long-term variability F-tests and therefore they will be discarded from discussion. The others will be discussed individually in Sect. 6.

5. Radial-velocity, activity and CCF parameters

Figure 1 shows the time-series of radial velocity, activity, and the CCF parameters' BIS, FWHM and contrast for the 27 stars that passed the selection criteria (before the variability F-tests). Small points are nightly averaged data used to calculate the bins, points with errorbars are the binned data (the errors are explained in Sect. 2). The peak-to-peak variation (Δ) and rms (σ) are also shown. The RV time-series have the known planetary companions' signal subtracted.

HIP38594 showed a trend in RV after removal of secular acceleration, with a slope of $-50.83 \pm 0.51 \text{ m s}^{-1} \text{ yr}^{-1}$. This corresponds to a variation of $\Delta(V_r) = 307.5 \text{ m s}^{-1}$ in our timespan and is probably due to a stellar companion. A Keplerian fit gives an orbit for a companion with a minimum period (only a linear trend is observed in the data) of 4941 ± 1516 days. Since we are only concerned with low-amplitude and long-term variations, we removed this trend.

Other stars appear to have linear trends in RV, such as Gl 205 (with $\Delta(V_r) = 9 \text{ m s}^{-1}$) and Gl 680 ($\Delta(V_r) = 15 \text{ m s}^{-1}$), but since these trends have lower amplitude variations we decided to keep them for the rest of the study (see Sect. 5.2 for more information).

5.1. Activity and radial-velocity scatter

Table 2 shows the radial-velocity rms after the subtraction of the orbits together with the mean and rms of the Na I index for the binned data of the full sample. The scatter in radial velocity, $\sigma_e(V_r)$, varies between 0.29 for Gl 849 and 5.9 m s^{-1} for Gl 680. The most active star in the sample is Gl 551 (Proxima Centauri) with an average Na I index of 0.49, while the most inactive star is Gl 699 (Barnard's star) with an average Na I value of 0.059 (but highest relative scatter in Na I with $\sim 14\%$). We should alert, however, that the average Na I index values depend on stellar color (see Fig. 6 of Paper I) and should not be used to compare activity between stars with different colors without having the index calibrated for the photospheric contribution and without being reported to the bolometric flux.

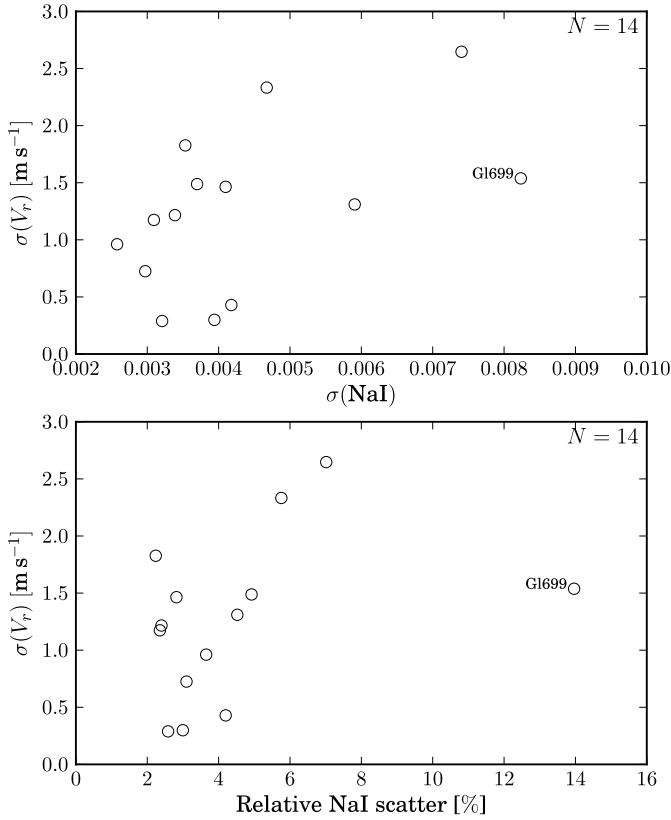
The most active star in the sample, Gl 551, also have the highest absolute scatter in Na I index (and 12% relative scatter). But its RV dispersion is not particularly high, having a standard deviation of $\sigma_e(V_r) = 1.5 \text{ m s}^{-1}$.

Meunier et al. (2010) simulated the effects of spots, plages, and inhibition of convection in the solar radial velocity during a solar activity cycle when the Sun is seen edge-on and observed as a star (integrated flux over the whole disk). The authors found that the signal induced by the three effects on the solar RV during the cycle had an rms of $\sigma(V_r) = 2.40 \text{ m s}^{-1}$, with a peak-to-peak variation of 10.6 m s^{-1} .

The median RV rms of 1.5 m s^{-1} for our sample is lower than the results of Meunier et al. (2010) and therefore in agreement with the extrapolation towards M dwarfs of Lovis et al.

Table 2: Statistics for RV and Na I, and probabilities $P(F)$ of the variability F-tests for activity. All parameters were calculated for the data with 150 day bins.

Star	N_{bins}	Sel.	$\sigma_e(V_r)$ [m s ⁻¹]	$\langle \sigma_r(V_r) \rangle$ [m s ⁻¹]	$\langle \text{Na I} \rangle$	$\sigma_e(\text{Na I})$	$\langle \sigma_r(\text{Na I}) \rangle$	$P(F)$
Gl 1	5	Yes	0.58	0.71	0.104	0.0021	0.0013	0.18
Gl 176	7	No	2.7	0.94	0.188	0.0074	0.0044	0.12
Gl 205	6	No	2.9	0.82	0.179	0.0046	0.0029	0.16
Gl 273	6	Yes	1.5	0.49	0.075	0.0037	0.0016	0.042
Gl 382	5	No	2.1	2.2	0.196	0.0052	0.0027	0.12
Gl 393	5	No	1.6	0.71	0.146	0.0037	0.0023	0.18
Gl 433	6	Yes	1.2	0.71	0.141	0.0034	0.0011	0.011
Gl 436	8	Yes	0.43	0.52	0.100	0.0042	0.0012	0.0017
Gl 479	4	No	2.0	0.97	0.186	0.0040	0.0029	0.31
Gl 526	4	No	1.8	0.69	0.158	0.0035	0.0011	0.042
Gl 551	6	No	1.5	0.83	0.493	0.057	0.044	0.28
Gl 581	13	Yes	0.96	0.51	0.071	0.0026	0.0013	0.012
Gl 588	5	Yes	1.3	0.39	0.131	0.0059	0.0010	0.0025
Gl 667 C	8	Yes	0.73	0.61	0.096	0.0030	0.0014	0.031
Gl 674	5	No	2.3	0.73	0.138	0.0037	0.0029	0.32
Gl 680	6	No	5.9	0.93	0.146	0.0048	0.0022	0.059
Gl 699	5	No	1.5	0.61	0.059	0.0082	0.0027	0.027
Gl 832	5	Yes	0.30	0.66	0.132	0.0039	0.0015	0.047
Gl 849	6	Yes	0.29	0.77	0.124	0.0032	0.0013	0.032
Gl 876	6	No	2.3	1.8	0.081	0.0047	0.0017	0.020
Gl 877	5	Yes	2.7	1.3	0.106	0.0074	0.0020	0.014
Gl 887	4	No	1.6	1.1	0.173	0.0038	0.0014	0.062
Gl 908	9	Yes	1.2	0.55	0.131	0.0031	0.0014	0.020
HIP12961	6	No	1.3	0.89	0.172	0.0028	0.0016	0.12
HIP19394	7	No	5.3	2.0	0.094	0.0033	0.0019	0.096
HIP38594	4	No	2.6	1.2	0.169	0.0058	0.0020	0.055
HIP85647	6	Yes	1.5	1.3	0.145	0.0041	0.0017	0.039


 Fig. 2: *Top*: Radial-velocity scatter versus Na I scatter. *Bottom*: Radial-velocity scatter versus relative Na I scatter.

(2011) results which found that later-type stars have lower amplitude RV influenced by long-term activity than earlier-type stars. It is expected that the stronger contribution to RV from magnetic activity cycles comes from the inhibition of convection (Meunier et al. 2010). Since cell convection structure is strongly depending on the effective temperature of the stars, the impact of their inhibition should be also depending of spectral type. Thus, it is expected that activity cycles will have different influence on RV for different types of stars. Furthermore, some of these stars may have undiscovered low-mass companions that could reduce the RV rms even further.

Figure 2 shows the rms variation of radial velocity against the rms of Na I index (top panel) and relative variation of Na I (lower panel). A relation between these parameters is clearly visible: stars with higher long-term scatter of activity also present higher long-term scatter in radial velocity. The minimum long-term relative variation we could detect in the Na I index was around 2%, with highest scatter reaching around 14%. Gl 699 appears to be an outlier, more evidently when we consider the relative activity values. Although this star has an average value of $\sigma(V_r)$ when compared to the rest of the sample, it has the highest relative activity variation, almost the two times the value of the star with the second highest relative activity variation.

5.2. Correlation between RV and activity

Table 3 shows the correlation coefficients of the relation between RV and Na I with the respective FAPs. The FAPs were calculated using bootstrapping of the nightly averaged data, followed by a re-binning and a subsequent determination of the correlation coefficient for each of the 10000 permutations (see also Paper I).

Table 3: Pearson correlation coefficients with respective FAPs.

Star	V_r vs Na I		Na I vs BIS		Na I vs FWHM		Na I vs Contrast	
	ρ	FAP	ρ	FAP	ρ	FAP	ρ	FAP
Gl 273	0.84	0.022	-0.64	0.094	0.60	0.13	-0.89	0.0074
Gl 433	0.91	0.0018	-0.70	0.11	0.70	0.031	-0.53	0.14
Gl 436	0.83	0.0091	0.28	0.29	0.82	0.0074	0.44	0.15
Gl 526	0.86	0.13	0.27	0.34	0.90	0.057	-0.76	0.13
Gl 581	0.24	0.25	0.11	0.38	0.60	0.019	-0.38	0.13
Gl 588	0.82	0.033	0.03	0.49	-0.51	0.24	-0.40	0.25
Gl 667C	0.45	0.12	-0.35	0.26	-0.27	0.22	0.37	0.17
Gl 699	0.32	0.31	-0.12	0.42	0.55	0.15	-0.79	0.070
Gl 832	-0.20	0.36	-0.41	0.30	0.57	0.19	0.08	0.46
Gl 849	-0.37	0.25	-0.38	0.26	0.69	0.097	-0.29	0.29
Gl 876	0.63	0.091	0.45	0.15	0.27	0.30	-0.15	0.39
Gl 877	0.77	0.11	-0.74	0.085	0.93	0.023	-0.45	0.21
Gl 908	0.85	0.0038	-0.61	0.051	0.82	0.0075	0.43	0.093
HIP85647	-0.03	0.48	0.32	0.30	0.81	0.039	-0.87	0.014

Notes. Only the 14 stars that passed the activity variability tests in Sect. 3 are considered. Bold highlights indicate FAP values lower than 0.05 (95% significance level). FAPs were calculated via bootstrapping as in Paper I.

The tendency for positive correlations is clear, with an average correlation coefficient of $\langle \rho \rangle = 0.49$. Five stars show a significant correlation coefficient (with $\leq 5\%$ false-alarm probability) between activity and radial velocity, which represents 36% of the sample. These stars are Gl 273, Gl 433, Gl 436, Gl 588, and Gl 908 and their coefficients range between 0.82 and 0.91. One more star, Gl 876, has a FAP value lower than 10%, with a correlation coefficient of 0.63. If a FAP lower than 10% is taken as the limit, then we have $\sim 43\%$ of the variable stars having their RV induced by long-term activity.

Fig. 3 shows the slope of the correlation between radial velocity and Na I index as a function of $(V - I)$ colour. Symbols are in three sizes dependent on the correlation coefficient values: large for $\rho \geq 0.75$, medium for $0.50 \leq \rho < 0.75$, and small for $\rho < 0.50$. The data points have three colors based on the FAP values: black for $\text{FAP} \leq 0.01$, grey for $0.01 < \text{FAP} \leq 0.05$, and white for $\text{FAP} > 0.1$. The errorbars are the errors on the slope. We can see in the figure that there is a clear tendency for positive slopes of the correlation RV–Na I. This implies that a positive change in activity will induce a positive change in the apparent stellar velocity.

All the cases of significant correlation have positive coefficients and the slopes of the correlation range from 85 to 338 $\text{m s}^{-1} \text{Na I}^{-1}$. Contrary to what Lovis et al. (2011) found for FGK stars, we found no strong relationship between the slopes and stellar colour (a proxy of T_{eff}) for this sample of early-M dwarfs. Furthermore, we found no cases of significant anti-correlations as could be expected from the author’s study. It can be that the author’s correlation observed in their Fig. 18 (lower panel) reaches a plateau for lower effective temperatures or that the variations induced by long-term activity on the RV of M dwarfs are so low that they are more difficult to observe (some of the observed scatter reaches the same level as the instrument precision). Another possibility could be that still undetected small planets might interfere with the radial-velocities and therefore ruin any hypothetical correlation.

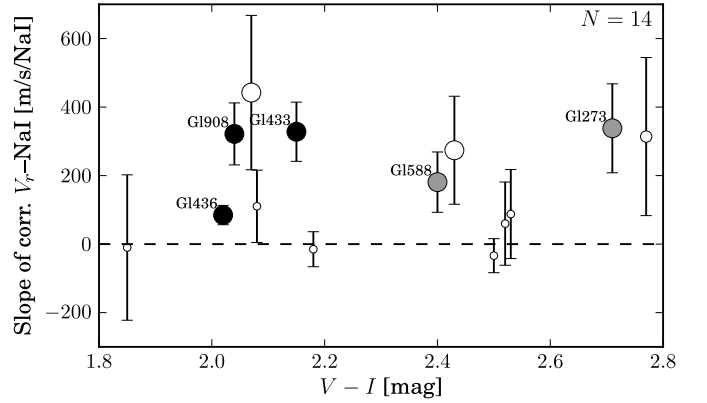


Fig. 3: Slope of the correlation between velocity and activity against $(V-I)$ color. Symbol sizes depend on the value of the correlation coefficient between RV and activity: large for $\rho \geq 0.75$, medium for $0.50 \leq \rho < 0.75$, and small for $\rho < 0.50$. The data points have three colors based on the FAP values: black for $\text{FAP} \leq 0.01$, grey for $0.01 < \text{FAP} \leq 0.05$, and white for $\text{FAP} > 0.1$. The errorbars are the errors on the slope.

5.3. Correlation between activity and the CCF parameters

5.3.1. Na I vs BIS

In this work we found a marginal tendency for negative correlations between Na I and BIS, with $\langle \rho \rangle = -0.18$. No cases of significant coefficients with $\text{FAP} \leq 5\%$. Three cases of marginal ($5\% < \text{FAP} \leq 10\%$) anti-correlation, Gl 273 with $\rho = -0.64$, Gl 877 with $\rho = -0.74$, and Gl 908 with $\rho = -0.61$ (21% of the sample). Due to the lack of significant cases of correlation with activity, the line bisector seems thus not to be a very good long-term activity indicator for early-M dwarfs.

This is different from the trend found between activity and BIS for early-K stars where the two were found to be positively correlated (e.g. Santos et al. 2010). While the BIS values found here were all negative, Santos et al. (2010) measured positive BIS values in all stars. Although the absolute value of BIS would increase with activity, for the case of negative values found in this study it means that the increase was a negative increase, and

therefore anti-correlated with activity. We can speculate that the difference in the signal of the BIS values might be attributed to, either the bisectores of K and M dwarfs having inverse shapes, or the use of different cross-correlation masks to obtain the CCF line profiles (see e.g. Dall et al. 2006).

5.3.2. Na I vs FWHM

We found a tendency for positive correlations between our activity indicator and width of the CCF profile, with $\langle \rho \rangle = 0.53$ (the strongest average correlation coefficient between parameters). Similarly, a positive trend was also found for early-K stars (e.g. Santos et al. 2010). And therefore we consider that the qualitative behaviour of FWHM with activity is similar for different spectral types, an effect also shown in Lovis et al. (2011). Six stars have strong correlations in the range 0.60–0.93 with $\text{FAP} \leq 1\%$ (which represent 43% of our 14-star sample). These are Gl 433, Gl 436, Gl 581, Gl 877, Gl 908, and HIP85647. Two more stars show marginal correlation, Gl 526 and Gl 849. If we count them, then 57% of our stars have long-term correlation between activity and FWHM. This means that the use of FWHM should be useful to detect long-term activity-like variations in M-dwarfs and can be used in complement to other activity proxies.

5.3.3. Na I vs contrast

As was detected by Santos et al. (2010) for earlier-type stars, we found a tendency for anti-correlation, $\langle \rho \rangle = -0.30$ between the activity level and the contrast of the CCF. But only two cases of significant coefficients, Gl 273 with $\rho = -0.89$ and HIP85647 with $\rho = -0.87$ were found. This represents only 14% of the sample, an indication that the depth of the CCF line is not an optimal measure of the activity level of M dwarfs (at least as measured by the Na I/Ca II lines). Two other cases of marginal correlation, Gl 699 with $\rho = -0.79$ and Gl 908 with $\rho = 0.43$ are present.

6. Individual cases

6.1. Stars with significant RV–activity correlation

Gl 273 This star shows the highest slope of the RV–activity relation of the stars with significant correlation. Its slope has a value of $328 \text{ m s}^{-1} \text{ Na I}^{-1}$ with the RV having a peak-to-peak variation of $\Delta = 5 \text{ m s}^{-1}$ and a rms of $\sim 1.5 \text{ m s}^{-1}$. Its RV–activity correlation coefficient is 0.84 with a FAP of 2% (Fig. 4). This star also presents a strong anti-correlation between Na I and contrast with $\rho = -0.89$ ($\text{FAP} = 0.0074$). A moderate anti-correlation is also observed between Na I and BIS ($\rho = -0.64$, $\text{FAP} = 0.094$). Although we found signs of correlation between activity and RV we were not able to properly fit a sinusoidal to the Na I time series.

Gl 433 In Paper I we found this star to present a maximum in activity, typical of cycle-type long-term activity variations. Figure 5 (middle and bottom panels) shows that the RV time-series, after removal of the planetary signal (Delfosse et al. 2012, in prep.), follows a similar pattern as the Na I index. The correlation coefficient between the two is $\rho = 0.91$ with a FAP of 0.0018 (Fig. 5, top panel). The Na I index also shows correlations with CCF parameters of -0.70 and 0.70 for BIS and FWHM respectively. We can therefore confirm that the activity cycle maximum

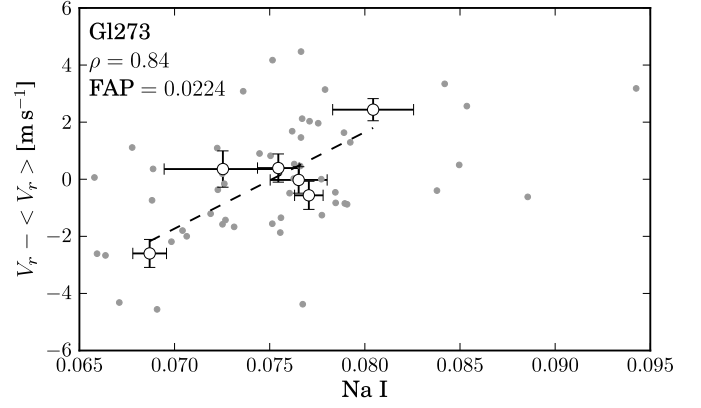


Fig. 4: Radial-velocity relation with Na I index for Gl 273. Small dots without errorbars are nightly averaged and points with errorbars are averaged over 150 days. The dashed line is the best linear fit. The correlation coefficient ρ and the respective FAP are shown.

is inducing a maximum in RV. The slope of the RV–Na I correlation is $328 \text{ m s}^{-1} \text{ Na I}^{-1}$ and we measured an overall variation in RV of 3.29 m s^{-1} (with $\sigma_e(V_r) = 1.22 \text{ m s}^{-1}$). The amplitude and period of the cycle in both Na I or RV scales cannot be inferred because we do not have an entire cycle period in our data. However, a minimum limit for the amplitude and period can be calculated by fitting a sinusoid to the activity time-series. We determined that the minimum activity cycle period is 1665 days with a minimum amplitude of 0.004 in Na I (Fig. 5, middle panel). A similar minimum period was also found for the radial velocity signal with a value of 1758 days and an amplitude of 1.45 m s^{-1} (Fig. 5, bottom panel). This star represents therefore a good example of an RV signal induced by an activity cycle.

Gl 436 This star has the smallest slope of the RV–activity correlation with a value of $85 \text{ m s}^{-1} \text{ Na I}^{-1}$. From Fig. 6 we can observe a large scatter in the nightly averaged data. Ballard et al. (2010) reported on short-term noise in photometry that they attributed to stellar spots. Furthermore, Knutson et al. (2011) detected evidence of occulted spots during the transits of Gl 436 b (Butler et al. 2004). It is probable that short-term activity variability is producing the large scatter in Na I and contributing to a reduction of the slope’s value. Nevertheless, the correlation coefficient of the RV–activity relation is $\rho = 0.83$ with a FAP of 0.9%, providing clues for the influence of long-term activity on the observed RV of the star. A strong correlation coefficient between Na I and FWHM of 0.82 ($\text{FAP} = 0.7\%$) was also found. However, we tried to fit a sinusoidal signal to both the RV and Na I time series but obtained no significant results. The activity time series in Fig. 1 shows a decreasing trend in activity that can be due to a long-period magnetic cycle, but more data will be needed to firmly prove this.

Gl 588 With a correlation coefficient of 0.82 ($\text{FAP} = 3.3\%$) this star also presents a strong long-term relationship between velocity and activity (Fig. 7). This correlation has a slope of $181 \text{ m s}^{-1} \text{ Na I}^{-1}$. The RV time series (Fig. 1) shows a periodic-like signal with a peak-to-peak variation of 3.6 m s^{-1} similar to the Na I time series apart from a point at $\text{BJD} \sim 2453560 \text{ d}$. This is a point which includes only four nights that might be influenced

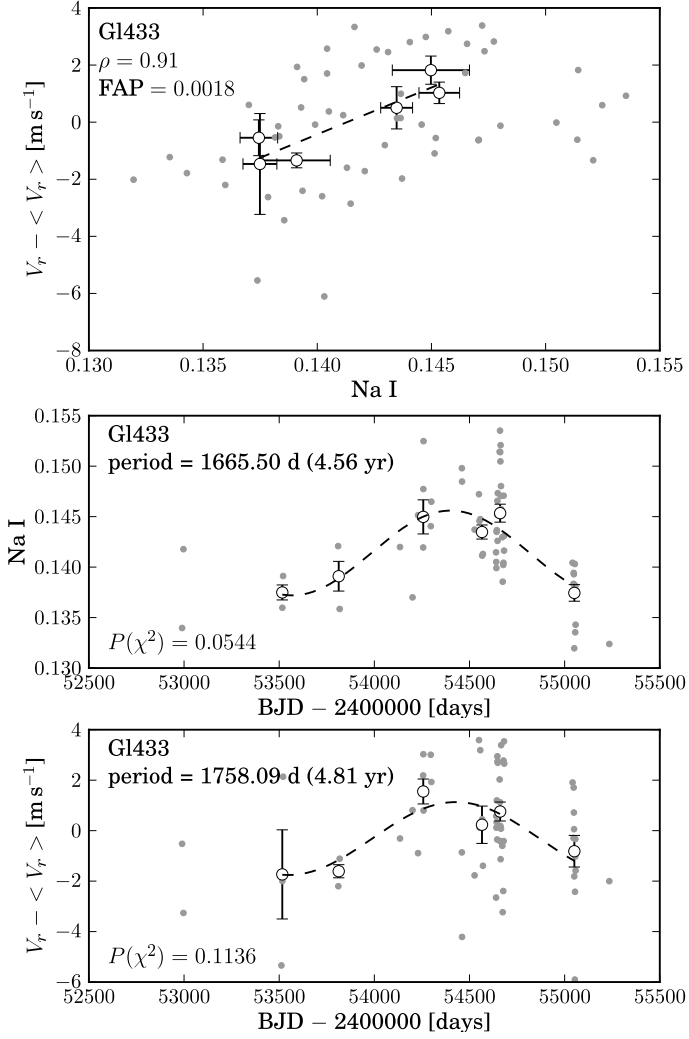


Fig. 5: *Top*: Radial-velocity relation with Na I index for Gl 433. *Middle*: sinusoidal fit to the Na I index for Gl 433. *Bottom*: Sinusoidal fit to RV of Gl 433. Small dots without errorbars are nightly averaged and points with errorbars are averaged over 150 days. The dashed lines represent the best linear (top) and sinusoidal (middle, bottom) fits to the data.

by short-term activity variability. It is therefore not possible to conclude about the periodicity of this stars' activity cycle.

Gl 908 This is another good example of long-term correlation between RV and activity. The correlation coefficient has a value of 0.85 (FAP = 0.4%) and the trend can be observed both in the binned and in the nightly averaged data (Fig. 8). The slope of the correlation is $322 \text{ m s}^{-1} \text{ Na I}^{-1}$ and we measured an RV peak-to-peak variation of 3.85 m s^{-1} . A strong correlation between Na I and FWHM with $\rho = 0.82$ (FAP = 0.75%) was also detected. Although we have strong evidence for RV induced by long-term activity, we could not fit a sinusoidal signal to both time series with significant $p(\chi^2)$. This star has probably a magnetic "cycle" with no determined period, i.e., a star with a long-term aperiodic magnetic activity variability (these types of variations were classified as *var* (variable) by Baliunas et al. 1995).

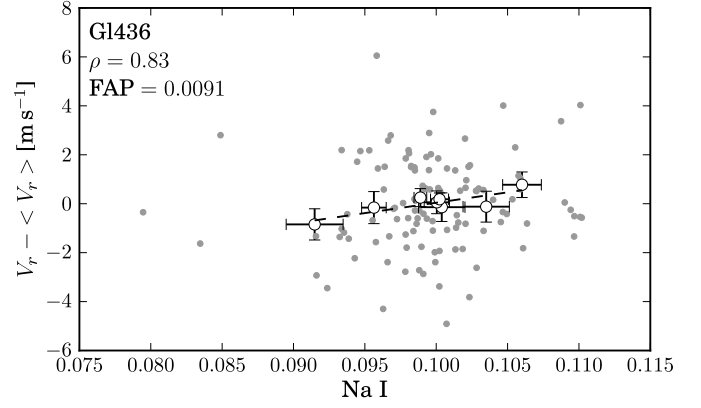


Fig. 6: Radial-velocity relation with Na I index for Gl 436. Small dots without errorbars are nightly averaged and points with errorbars are averaged over 150 days. The dashed line is the best linear fit. The correlation coefficient ρ and the respective FAP are shown.

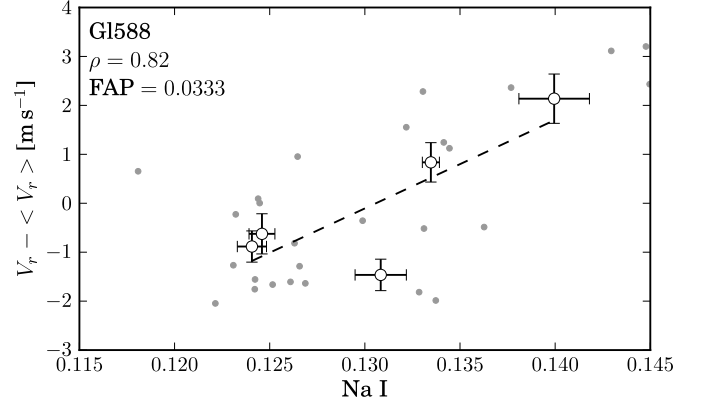


Fig. 7: Radial-velocity relation with Na I index for Gl 588. Small dots without errorbars are nightly averaged and points with errorbars are averaged over 150 days. The dashed line is the best linear fit. The correlation coefficient ρ and the respective FAP are shown.

6.2. Other interesting cases

Gl 176 This star has what appears to be a long-term periodic signal with $P \sim 2043 \text{ d}$ in RV (see time-series plot Fig. 1). The same trend is not observed in the Na I index and it did not pass the variability tests. This star has a confirmed planetary companion, Gl 176 b with $P = 8.7 \text{ d}$, and a rotationally modulated activity signal with a period of $P = 39 \text{ d}$ (Forveille et al. 2009). But none of these signals can explain the $\sim 2000 \text{ d}$ variation. It can be due to a long-period yet undiscovered planet.

Gl 581 This is the star which has the best probability of having the activity data fitted by a periodic sinusoidal signal instead of a linear trend. We obtained a signal with a period of $P = 3.85 \text{ years}$ ($P(\chi^2) = 0.01\%$) and our timespan for this star is long enough to cover more than one activity cycle period (Fig. 9). Furthermore, Gl 581 also passed the variability tests. To date, four planets are known to orbit the star with two more planets that were discarded (Bonfils et al. 2005; Udry et al. 2007; Mayor et al. 2009; Forveille et al. 2011a). We removed the signal of the four confirmed planets which resulted in a long-term RV rms of 0.96

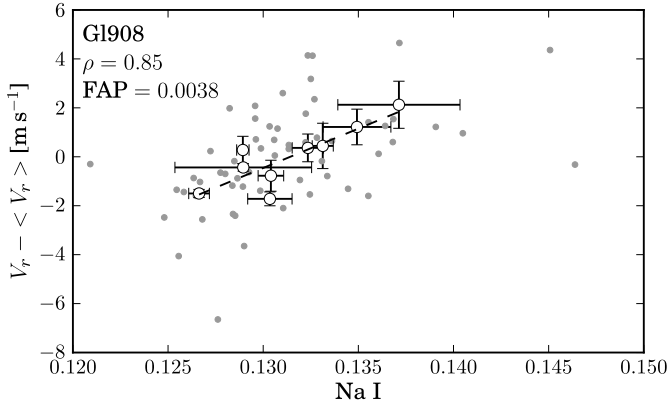


Fig. 8: Radial-velocity relation with Na I index for Gl 908. Small dots without errorbars are nightly averaged and points with errorbars are averaged over 150 days. The dashed line is the best linear fit. The correlation coefficient ρ and the respective FAP are shown.

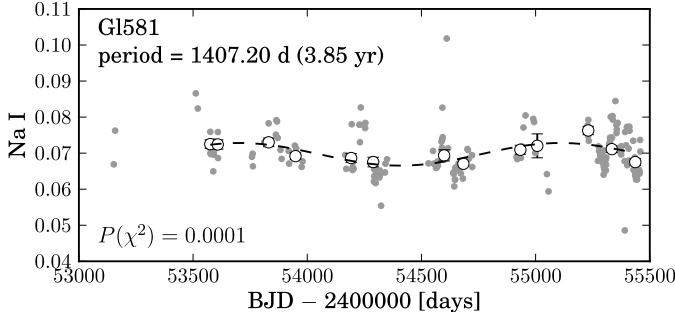


Fig. 9: Sinusoidal fit to the activity time series of Gl 581.

m s^{-1} which is of the order of the instrument precision. No correlation was found between long-term velocity and activity but the Na I index is correlated with FWHM ($\rho = 0.60$, FAP = 1.9%). Because of the large number of detected planets, it is sensible to recognise that their orbits might not have been properly subtracted from the data. We will therefore not take any conclusions about the possibility of the activity cycle being influencing the RV signal of this star.

Gl 667C One planet is known to orbit this star (Delfosse et al. 2012, in prep.). It is also a member of a triple system and orbits the A + B binary system. This system introduces a trend in RV that was subtracted together with the planetary companion signal. The Na I activity index passed the variability F-test and a sinusoidal function with a period of $P = 3.18$ years is well fitted to the activity time series (with $P(\chi^2) = 3.3\%$, Fig. 10). However, the RV signal is only marginally correlated with activity, having a correlation coefficient of $\rho = 0.45$ with a FAP of 12%. No correlations between the other parameters are detected.

Gl 699 Kürster et al. (2003) found an anti-correlation between RV and the $H\alpha$ index for the Bernard’s star with a coefficient of $\rho = -0.50$. Using a longer timespan for the same star, Zechmeister et al. (2009) detected a similar correlation with $\rho = -0.42$. We found only a marginal positive correlation with the Na I index ($\rho = 0.32$, FAP = 0.32). The Na I index of this

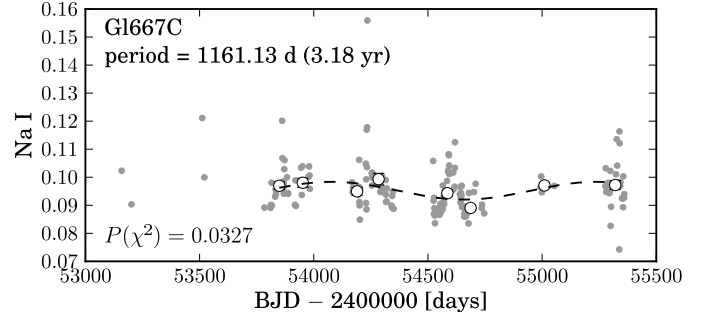


Fig. 10: Sinusoidal fit to the activity time series of Gl 667 C.

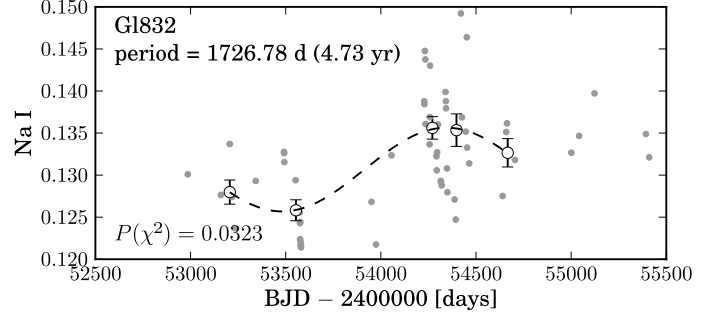


Fig. 11: Sinusoidal fit to the activity time series of Gl 832.

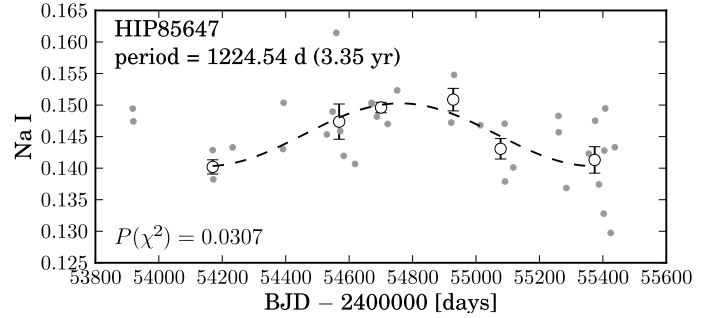


Fig. 12: Sinusoidal fit to the activity time series of HIP85647.

star is moderately correlated with both FWHM ($\rho = 0.55$, FAP = 0.15) and contrast ($\rho = -0.79$, FAP = 0.070).

Gl 832 This star passed the activity variability tests but we found no correlation with radial velocity after the removal of the planetary companion (Bailey et al. 2009). None of the other parameters are correlated apart from a marginal correlation between activity and FWHM of $\rho = 0.57$ but with a high FAP of 19%. The activity time series is well fitted by a sinusoidal function with $P(\chi^2) = 3.2\%$ and a minimum period of 4.73 years (Fig. 11).

HIP85647 After removal of the signal of the planetary companion (Forveille et al. 2011b) of this star and a linear trend due to a stellar companion, we found no correlation between RV and activity. There are strong correlations between Na I and the CCF parameters FWHM and contrast with $\rho = 0.81$ (FAP = 3.9%) and $\rho = -0.87$ (FAP = 1.4%), respectively. We successfully fitted a sinusoidal signal to the activity time series and obtained a period of 2.74 years (with $P(\chi^2) = 3.4\%$, Fig. 12).

7. Conclusions

We used a sample of 27 M0 to M5.5 dwarfs to study the relationship between long-term activity, radial velocity, and parameters of the cross-correlation function given by the HARPS pipeline. As the indicator for activity level we used the Na I index as suggested in Paper I. We binned the data to 150-day bins to average out high-frequency noise and removed any RV signals induced by known stellar or planetary companions.

A selection of stars having long-term activity variability was carried out by using F-tests. This resulted in a subsample of 14 variable stars, which means that around half of the stars in our sample have significant long-term activity variations.

The activity time series of some stars were fitted by sinusoidal functions to infer the activity cycle's period or minimum period. Five stars could be statistically well fitted by sinusoids and the inferred periods varied between 2.8 and 4.7 years. We should note, however, that our data covered close to one period or less of the fitted signals and therefore the cyclic nature of the signals cannot be fully established. Even if these stars have cyclic activity variability the periods obtained by the sinusoidal fitting should be regarded as minimum periods since the timespan is not long enough to cover two periods.

We obtained long-term velocity rms in the range 0.30 to 5.9 m s^{-1} and a relative scatter in Na I index for the 14-star variable subsample was in the range $\sim 2\text{--}14\%$. These two parameters, $\sigma(V_r)$ and $\sigma(\text{Na I})$, appear to be correlated. The median RV rms of 1.5 m s^{-1} that can possibly be induced by activity is lower than the one obtained for the case of the Sun by Meunier et al. (2010) as predicted by extrapolation of the trend in Fig. 18 (lower panel) of Lovis et al. (2011) for late-type stars.

We then searched for correlations between RV, activity and the CCF parameters BIS, FWHM, and contrast. The main general results we obtained can be summarised as:

- We found a general tendency for positive correlations between long-term activity and radial velocity variations. No relation between the slope of the correlation and stellar color was found.
- Five out of 14 stars with long-term variability have significant correlation between activity and radial velocity. This amounts to 36% of our subsample. These stars are Gl 273, Gl 433, Gl 436, Gl 588, and Gl 908. The maximum peak-to-peak RV variation we obtained for stars with significant correlation between long-term activity and RV was $\sim 5 \text{ m s}^{-1}$. Only Gl 433 had its activity well fitted by a sinusoidal signal even though the signal spans less than a full period. We determined a minimum period of 4.6 years for the activity cycle of this star, and similar minimum period of 4.8 years was found for the RV signal. The other stars could have aperiodic activity cycles but more data is needed to confirm this hypothesis.
- Although we found a general tendency for BIS to be anti-correlated with activity, those correlations were not statistically significant. Only 21% of the stars with long-term variability showed marginal correlations between activity and BIS. While we found a general trend for anti-correlations between activity and BIS for M dwarfs, Santos et al. (2010) found positive correlations between the S_{MW} activity index and BIS for early-K stars. This is a curious result that should be investigated further.
- We found that the long-term activity level was in general well correlated with FWHM. 43% of the stars with long-term variability had their activity level significantly correlated with FWHM. This is a good indication that the width

of the CCF profile can be used to follow long-term activity in M dwarfs, as a complement to activity indices. A similar result was found previously for the case of early-K dwarfs by Santos et al. (2010).

- When compared with activity, the contrast showed a tendency for negative correlations with only 14% of significant cases. The tendency for anti-correlations was also found by Santos et al. (2010) for early-K dwarfs, but since the fraction of significant coefficients is very low, this parameter does not seem to be a strong tool to diagnose long-term activity variability.

We found some cases of radial velocity variations induced by long-term activity. However, this does not seem to be a general trend. This can be due to several reasons including the bad frequency sampling of observations (since this is a program dedicated to the search of planets, most of the observations were focused on short-term RV variability to find short-period planets or with bad high-frequency sampling when the aim was to detect long-period companions), short timespan of the data (although we found some activity cycle periods to be of the 3-year order some could have periods longer than the ~ 6 -year span of our observations), and the fact that some of the stars might probably have low-mass and/or long-period planets not yet detected (and thus their RV signal could be adding confusion to our activity study). A longer timespan of observations will certainly contribute to a better understanding of how long-term activity cycles influence the detected velocity of these late-type stars.

In light of these results we must advise planet hunters to carefully check for long-term activity variations when faced with long-timespans of RV data since activity cycles could be adding noise or even mimicking the low-amplitude ($\leq 5 \text{ m s}^{-1}$) signals of planetary companions.

Acknowledgements. This work has been supported by the European Research Council/European Community under the FP7 through a Starting Grant, as well as in the form of a grant reference PTDT/CTE-AST/098528/2008, funded by Fundação para a Ciência e a Tecnologia (FCT), Portugal. J.G.S. would like to thank the financial support given by FCT in the form of a scholarship, namely SFRH/BD/64722/2009. N.C.S. would further like to thank the support from FCT through a Ciência 2007 contract funded by FCT/MCTES (Portugal) and POPH/FSE (EC).

References

- Bailey, J., Butler, R. P., Tinney, C. G., et al. 2009, *ApJ*, 690, 743
 Baliunas, S. L., Donahue, R. A., Soon, W. H., et al. 1995, *ApJ*, 438, 269
 Ballard, S., Christiansen, J. L., Charbonneau, D., et al. 2010, *ApJ*, 716, 1047
 Boisse, I., Bouchy, F., Hébrard, G., et al. 2011, *A&A*, 528, A4+
 Boisse, I., Moutou, C., Vidal-Madjar, A., et al. 2009, *A&A*, 495, 959
 Bonfils, X., Delfosse, X., Udry, S., et al. 2011, submitted
 Bonfils, X., Forveille, T., Delfosse, X., et al. 2005, *A&A*, 443, L15
 Bonfils, X., Mayor, M., Delfosse, X., et al. 2007, *A&A*, 474, 293
 Buccino, A. P., Díaz, R. F., Luoni, M. L., Abrevaya, X. C., & Mauas, P. J. D. 2011, *AJ*, 141, 34
 Butler, R. P., Vogt, S. S., Marcy, G. W., et al. 2004, *ApJ*, 617, 580
 Cincunegui, C., Díaz, R. F., & Mauas, P. J. D. 2007, *A&A*, 461, 1107
 Dall, T. H., Santos, N. C., Arentoft, T., Bedding, T. R., & Kjeldsen, H. 2006, *A&A*, 454, 341
 Díaz, R. F., Cincunegui, C., & Mauas, P. J. D. 2007a, *MNRAS*, 378, 1007
 Díaz, R. F., González, J. F., Cincunegui, C., & Mauas, P. J. D. 2007b, *A&A*, 474, 345
 Dumusque, X., Lovis, C., Ségransan, D., et al. 2011a, *ArXiv e-prints*
 Dumusque, X., Udry, S., Lovis, C., Santos, N. C., & Monteiro, M. J. P. F. G. 2011b, *A&A*, 525, A140+
 Endl, M., Kürster, M., Els, S., et al. 2002, *A&A*, 392, 671
 ESA. 1997, *VizieR Online Data Catalog*, 1239, 0
 Forveille, T., Bonfils, X., Delfosse, X., et al. 2011a, *ArXiv e-prints*
 Forveille, T., Bonfils, X., Delfosse, X., et al. 2009, *A&A*, 493, 645
 Forveille, T., Bonfils, X., Lo Curto, G., et al. 2011b, *A&A*, 526, A141

Gomes da Silva, J., Santos, N. C., Bonfils, X., et al. 2011, A&A, 534, A30+
Hawley, S. L., Gizis, J. E., & Reid, I. N. 1996, AJ, 112, 2799
Knutson, H. A., Madhusudhan, N., Cowan, N. B., et al. 2011, ApJ, 735, 27
Koen, C., Kilkenny, D., van Wyk, F., & Marang, F. 2010, MNRAS, 403, 1949
Kürster, M., Endl, M., Rouesnel, F., et al. 2003, A&A, 403, 1077
Lovis, C., Dumusque, X., Santos, N. C., et al. 2011, ArXiv e-prints
Mayor, M., Bonfils, X., Forveille, T., et al. 2009, A&A, 507, 487
Mayor, M., Marmier, M., Lovis, C., et al. 2011, ArXiv e-prints
Melo, C., Santos, N. C., Gieren, W., et al. 2007, A&A, 467, 721
Meunier, N., Desort, M., & Lagrange, A.-M. 2010, A&A, 512, A39+
Moutou, C., Mayor, M., Lo Curto, G., et al. 2011, A&A, 527, A63+
Queloz, D., Bouchy, F., Moutou, C., et al. 2009, A&A, 506, 303
Queloz, D., Henry, G. W., Sivan, J. P., et al. 2001, A&A, 379, 279
Saar, S. H. & Donahue, R. A. 1997, ApJ, 485, 319
Saar, S. H. & Fischer, D. 2000, ApJ, 534, L105
Santos, N. C., Gomes da Silva, J., Lovis, C., & Melo, C. 2010, A&A, 511, A54+
Santos, N. C., Mayor, M., Naef, D., et al. 2000, A&A, 361, 265
Ségransan, D., Mayor, M., Udry, S., et al. 2011, ArXiv e-prints
Udry, S., Bonfils, X., Delfosse, X., et al. 2007, A&A, 469, L43
Zechmeister, M., Kürster, M., & Endl, M. 2009, A&A, 505, 859

List of Objects

'Gl 1' on page 3
'Gl 176' on page 3
'Gl 205' on page 3
'Gl 273' on page 3
'Gl 382' on page 3
'Gl 393' on page 3
'Gl 433' on page 3
'Gl 436' on page 3
'Gl 479' on page 3
'Gl 526' on page 3
'Gl 551' on page 3
'Gl 581' on page 3
'Gl 588' on page 3
'Gl 667' on page 3
'Gl 674' on page 3
'Gl 680' on page 3
'Gl 699' on page 3
'Gl 832' on page 3
'Gl 849' on page 3
'Gl 876' on page 3
'Gl 877' on page 3
'Gl 887' on page 3
'Gl 908' on page 3
'HIP12961' on page 3
'HIP19394' on page 3
'HIP38594' on page 3
'HIP85647' on page 3

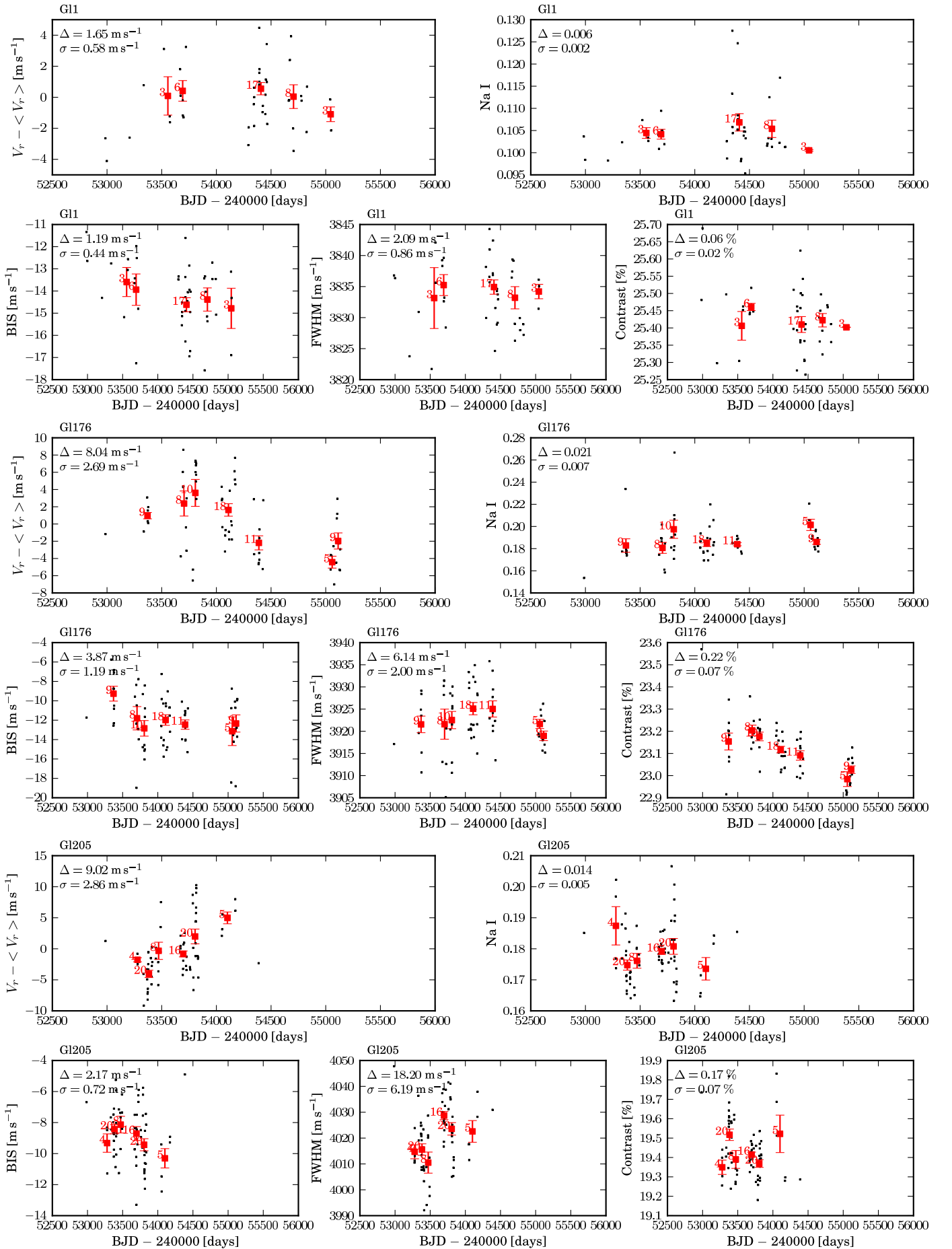


Fig. 1: Time-series of radial-velocity, Na I index, and BIS, FWHM, and contrast of the CCF line profile.

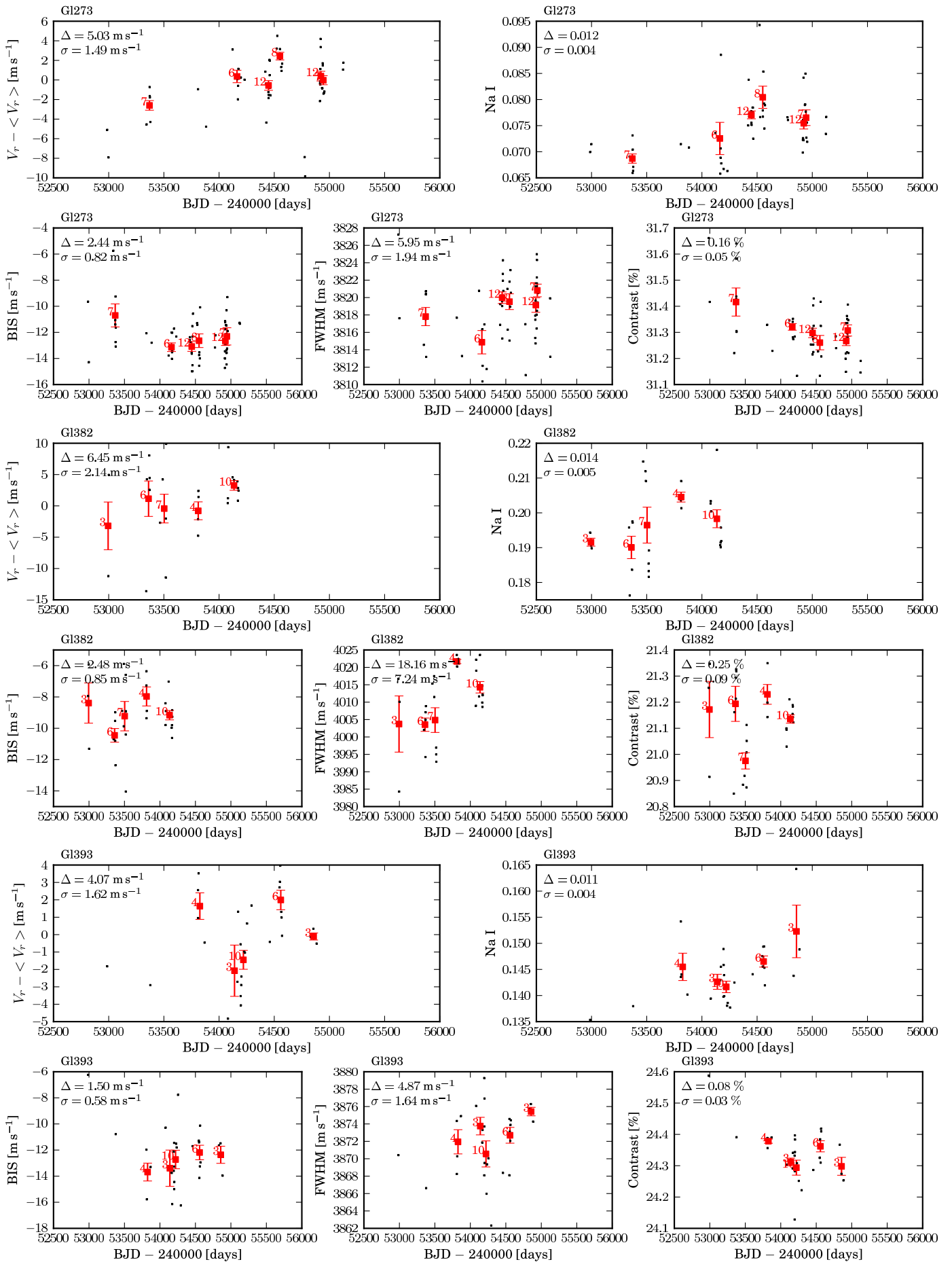


Fig. 1: Continued.

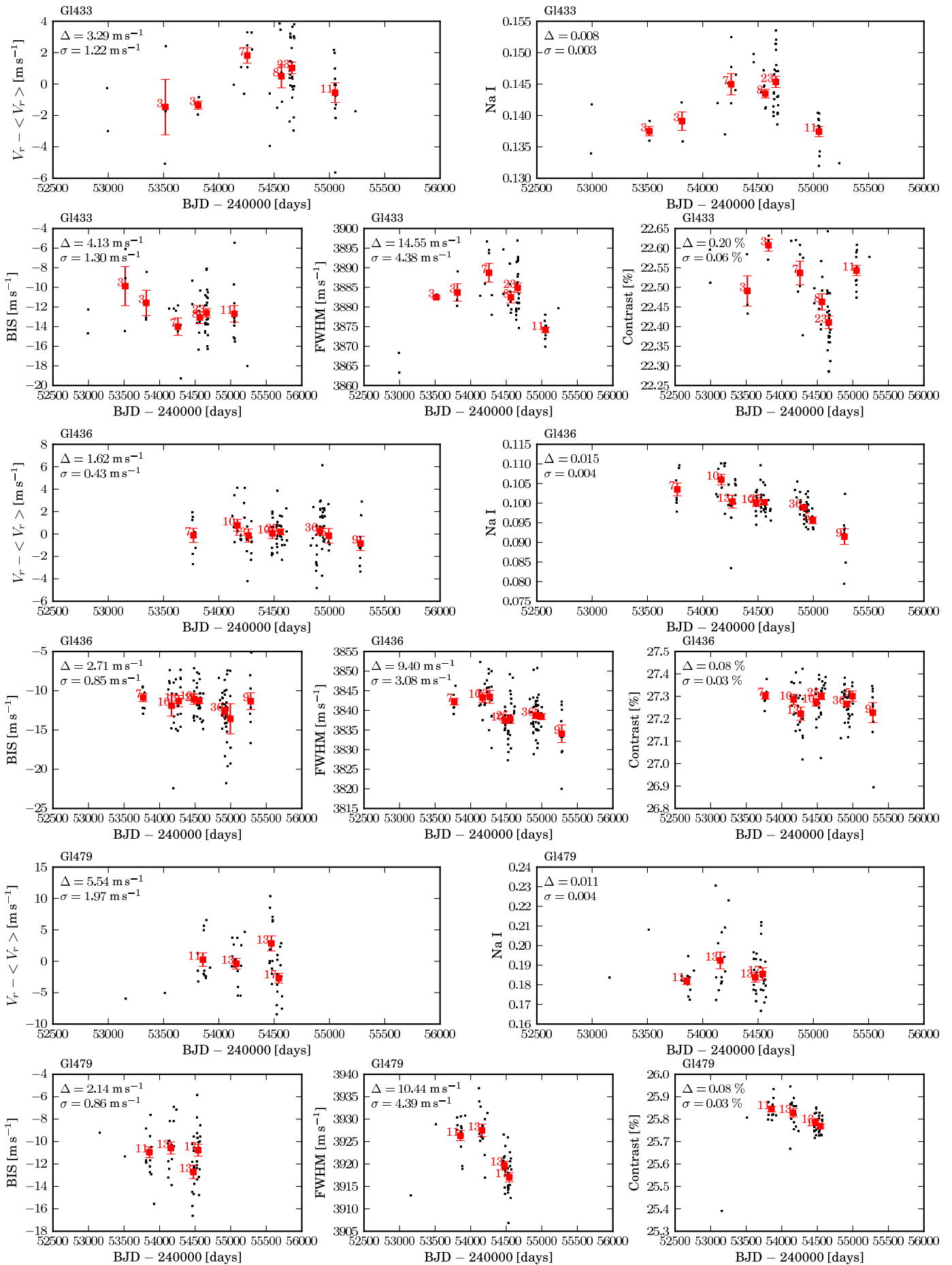


Fig. 1: Continued.

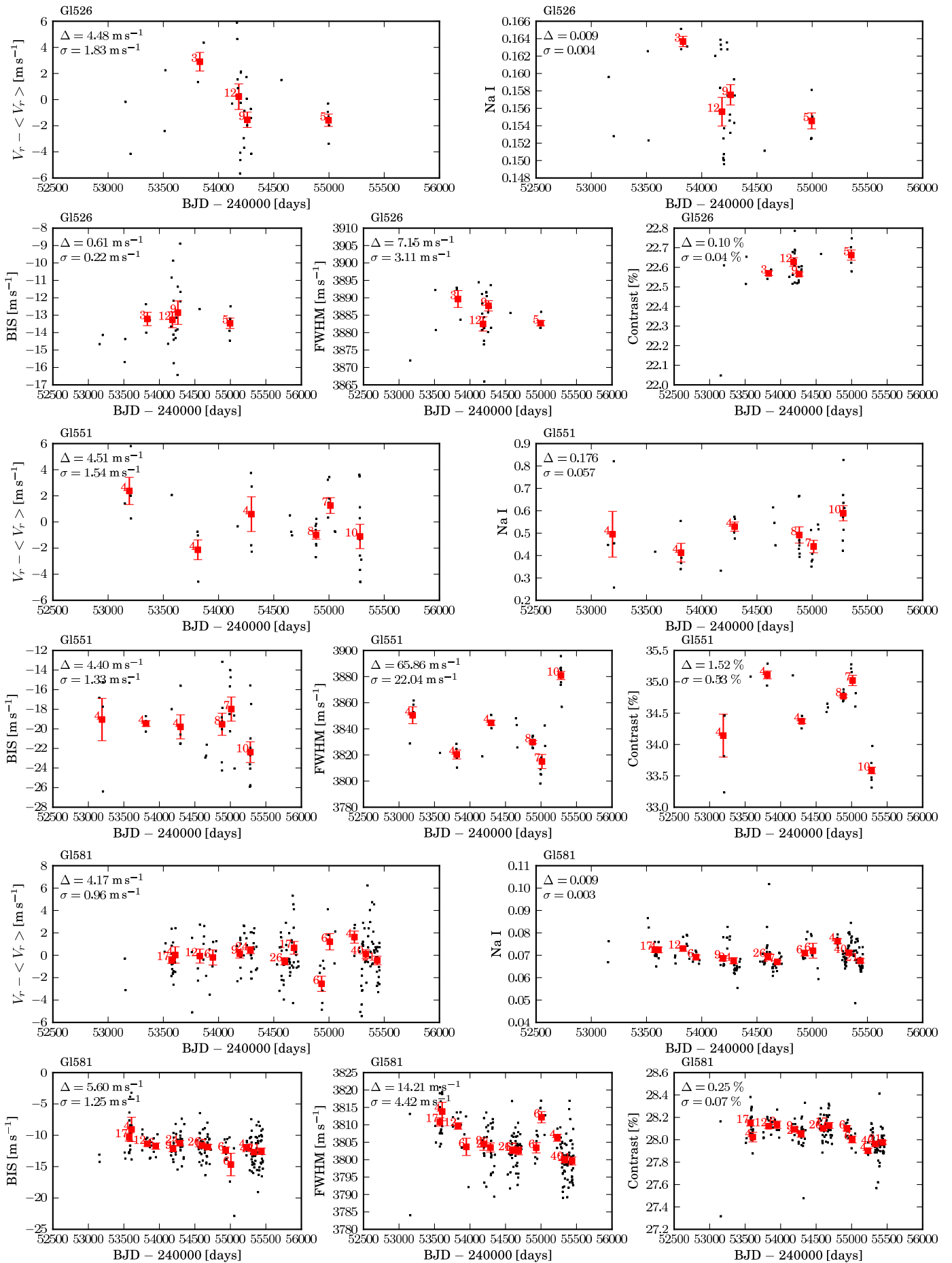


Fig. 1: Continued.

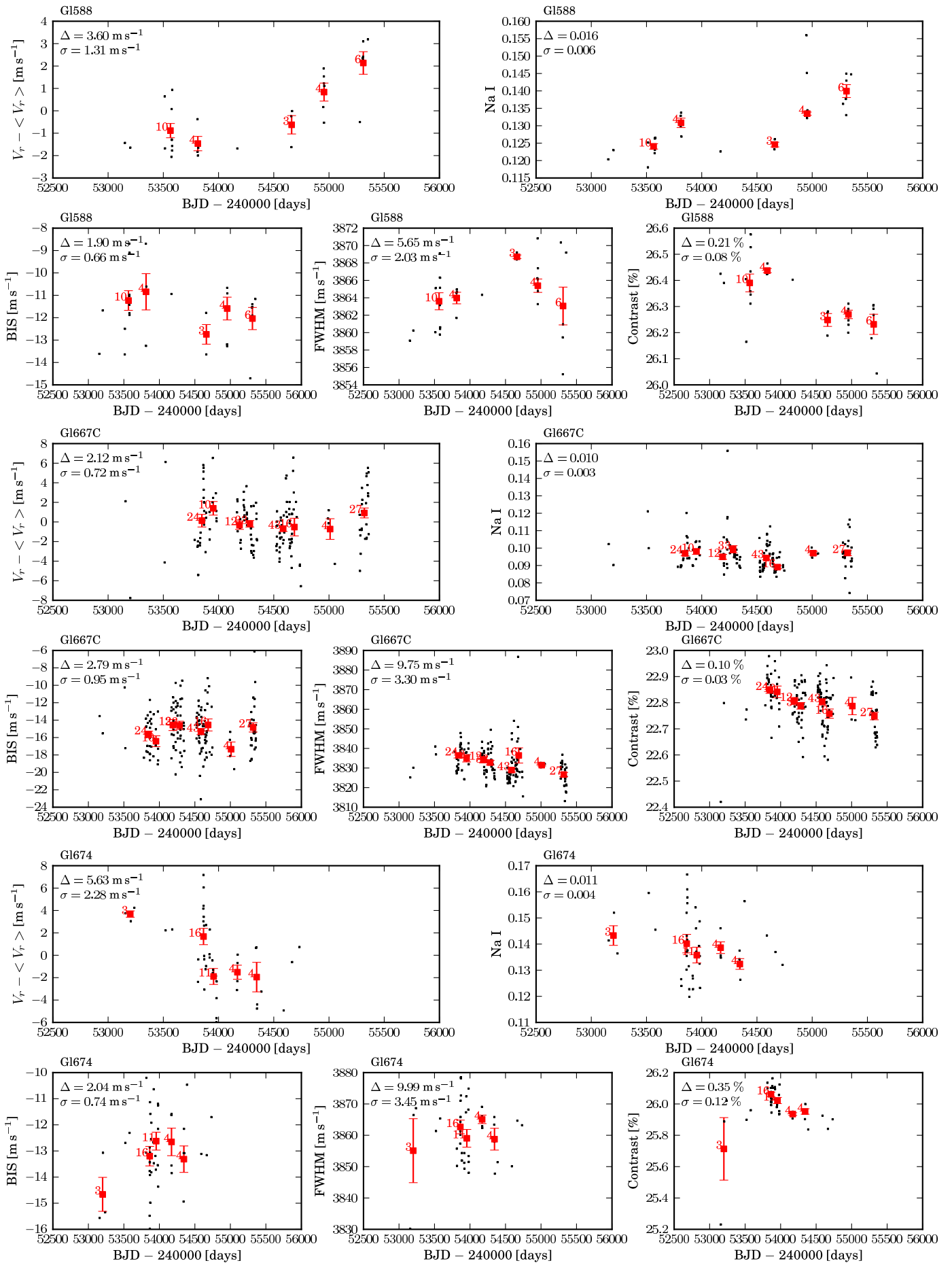


Fig. 1: Continued.

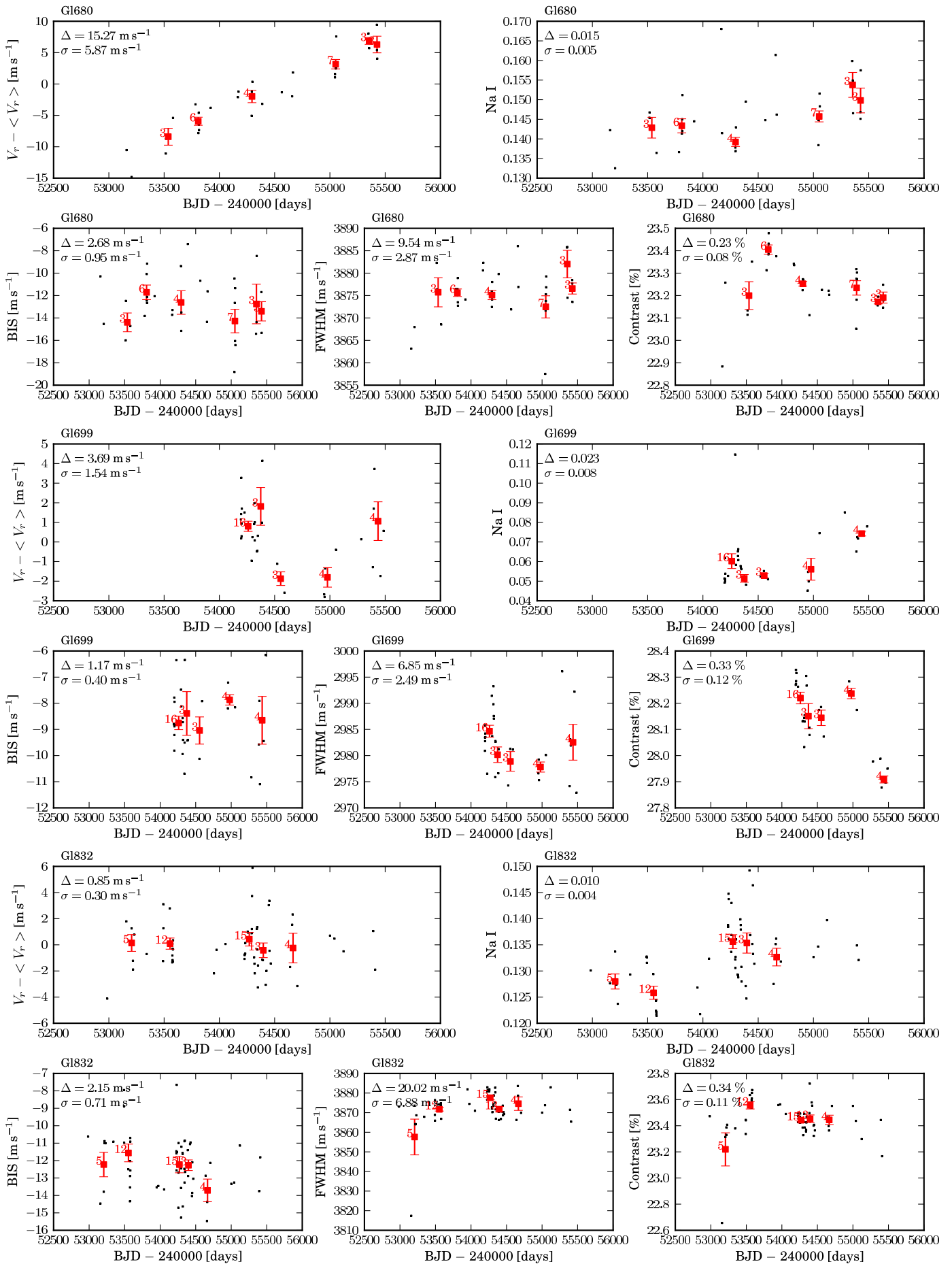


Fig. 1: Continued.

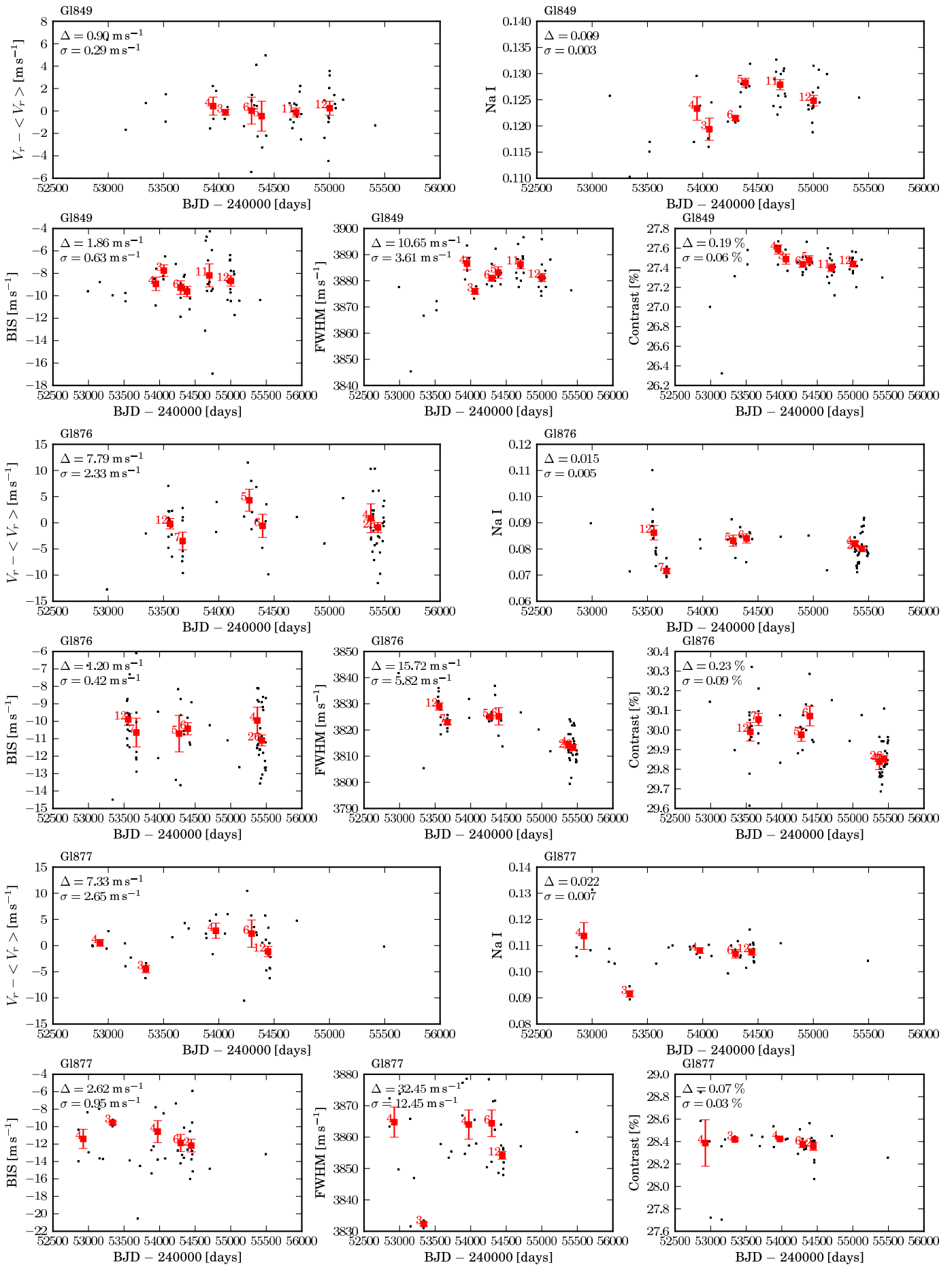


Fig. 1: Continued.

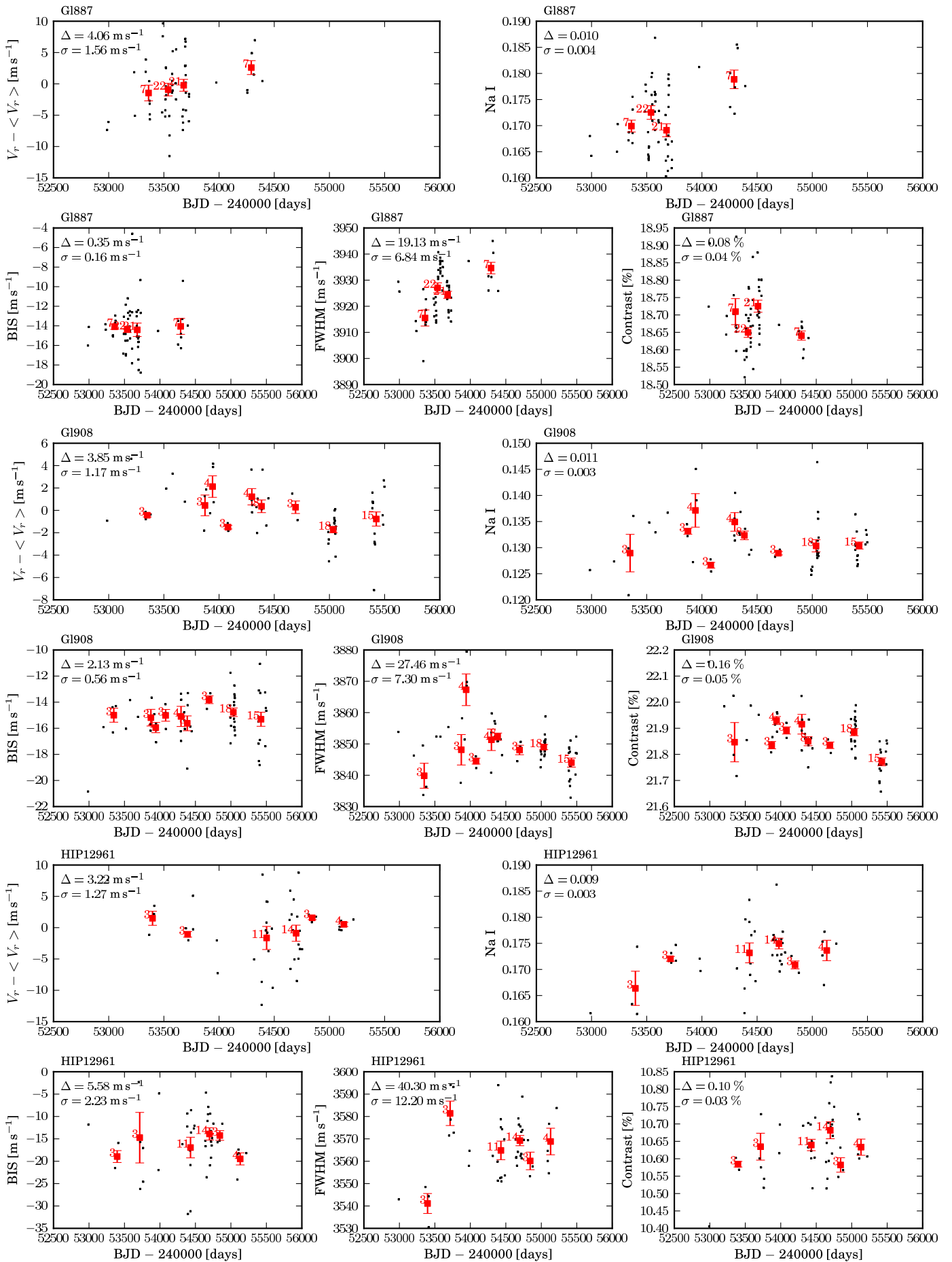


Fig. 1: Continued.

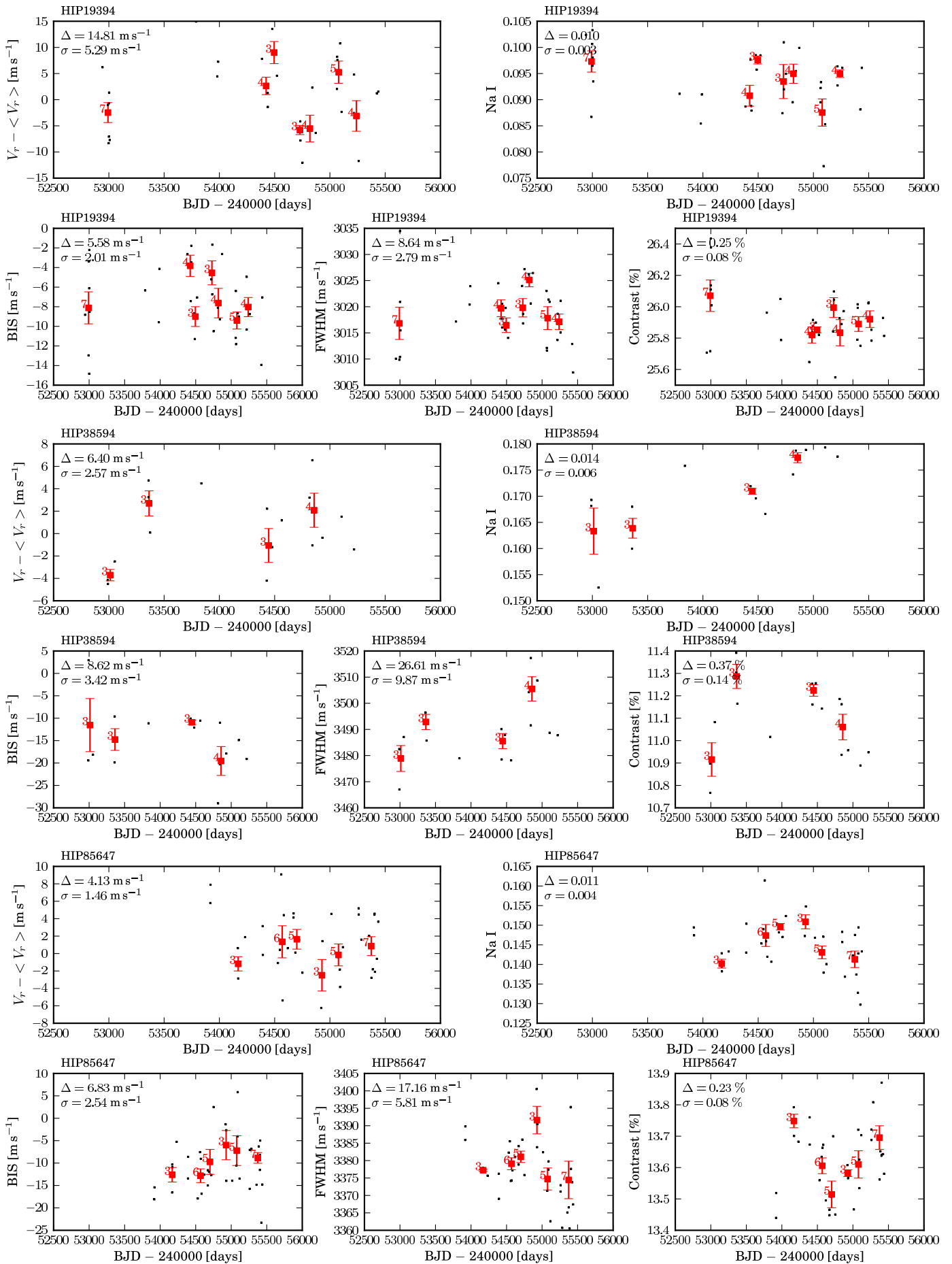


Fig. 1: Continued.